ACS APPLIED MATERIALS & INTERFACES

Research Article

www.acsami.org

Geometry-Controllable Graphene Layers and Their Application for Supercapacitors

Soojeong Lee,[†,⊥] Sang Ha Lee,[‡,⊥] Tae Hyung Kim,[‡,§] Misuk Cho,[‡] Ji Bum Yoo,[†] Tae-il Kim,*[,‡,§] and Youngkwan Lee*[,†,‡]

[†]Sungkyunkwan Advanced Institute of Nanotechnology (SAINT), Sungkyunkwan University (SKKU), 440-746 Suwon, Republic of Korea

[‡]School of Chemical Engineering, Sungkyunkwan University (SKKU), 440-746 Suwon, Republic of Korea

[§]Center for Neuroscience Imaging Research (CNIR), Institute for Basic Science (IBS), 440-746 Suwon, Republic of Korea

Supporting Information

ABSTRACT: A facile and ultrafast method for geometry controllable and vertically transformative 3D graphene architectures is demonstrated. The 2D stacked graphene layers produced by exfoliation of graphite were transformed, e.g., from horizontal to vertical, by applying electric charge (−2 V with 1−3 μAh/cm^2). The three-dimensionally transformed graphene layers have maximized surface area as well as high specific capacitance, 410 F g^{-1} in $LiClO_4$/PC electrolyte, which is 4.4 times higher than that of planar (stacked) graphene layers. Furthermore, they can remarkably exhibit 87% of retained capacitance as the scan rate is increased from 100 to 1000 mV s^{-1}, unlike planar graphene, which displays 61% retention under the same conditions.

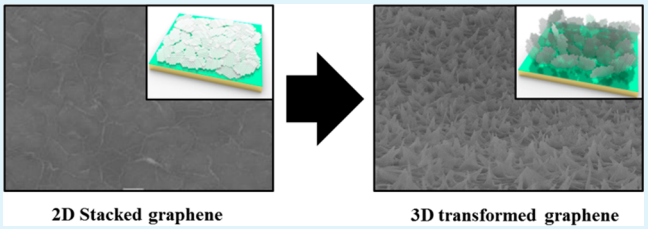

KEYWORDS: *graphene, geometry control, polystyrene sulfonate (PSS), supercapacitor*

INTRODUCTION

Graphene, a two-dimensional (2D) material composed of monatomic carbon atoms, has attracted great attention due to its superior electrical, optical, and thermal conductivities, as well as its mechanical properties.[1−3] It can be obtained through low cost processes such as the exfoliation of graphite or the reduction of graphene oxide[4−7] in addition to chemical vapor deposition (CVD) on metallic templates.[8,9] As such, graphene is a promising key component for future electronics, suitable for flexible electronics,[10] energy storage,[11] nanocomposite,[12] and many other applications.[13] Nevertheless, it falls short of expectations due to its limited geometry, i.e., intrinsically 2D structures.

Not long ago, in attempts to overcome the limitations of the geometrical structure of 2D graphenes and enlarge surface area of the graphene electrode for electronic devices as mentioned above, several methods for developing three-dimensional (3D) structured graphene and graphene oxide (GO) were presented. These methods include porous foam shape 3D carbon films,[14−17] fibered structures with carbon composite,[18] a hand rolling and skiving method,[19] mechanically wrinkled graphene film,[20] and patterning on a structured template.[21] However, they all have serious limitations like noncontrollable geometries,[15,21] polymeric binder or metallic nanoparticles impurities,[17] and require very complicated multistep fabrication processes.[14,18−20] Therefore, a simple fabrication method for geometry controllable graphene layers is necessary for the crucial applications.

Here we demonstrate a facile and ultrafast method for geometry controllable, vertically transformative 3D graphene architectures. The 2D stacked graphene layers produced by exfoliation of graphite were transformed, e.g., from horizontal to vertical, by applying electric charge (−2 V with 1−3 μAh/cm^2). The three-dimensionally transformed graphenes have maximized surface area as well as high specific capacitance, 410 F g^{-1} in $LiClO_4$/PC electrolyte, which is 4.4 times higher than that of planar (stacked) graphenes. Furthermore, they can remarkably exhibit 87% of retained capacitance as the scan rate is increased from 100 to 1000 mV s^{-1}, unlike planar graphene, which displays 61% retention under the same conditions. We also report here optimized deposition condition for shape-controllable graphene layers, so that the method will be useful in many other related applications.

EXPERIMENTAL SECTION

Preparation of Graphene/Polystyrene Sulfonate (PSS) Film. Polystyrene sulfonate sodium salt (PSS-Na, Mw = 70 000, Aldrich), ethanol (>98%, Samchun), nitric acid (HNO_3, 63%, Daejung), propylene carbonate (PC, 99%, Aldrich), and lithium perchlorate ($LiClO_4$, 98%, Aldrich) were used as received. Expanded graphite was prepared by thermal expansion from graphite (ash content < 0.05 mass %, particle size 200−300 μm, Zaval'evsk coal field, Ukraine), which was fluorinated by intercalation of C_2FnClF_3.[22] e-Graphite was treated

Received: January 21, 2015
Accepted: April 2, 2015
Published: April 2, 2015

DOI: 10.1021/acsami.5b00630
ACS Appl. Mater. Interfaces 2015, 7, 8070−8075

with nitric acid for 5 min to produce doped graphite. The doped graphite (1 mg) was dispersed in ethanol (100 mL), and the mixture was sonicated using a tip (bar type) sonication instrument at 750 W for 1 h in order to produce stable doped graphene dispersion. PSS film was prepared by dip-coating a gold electrode (0.28 cm^2) using 10 wt % PSS aqueous solution. The prepared PSS film was immersed in the graphene dispersed solution for 3 min to accumulate a graphene layer. After the process, the graphene deposited PSS film was dried at room temperature for 1 h.

Vertical Alignment of Graphene. Vertical alignment of graphene on PSS film was initiated by applying potential at −2 V with 0.001−0.003 mAh/cm^2 in HNO_3/ethanol (pH 4.0) electrolyte. The process was performed in a three-cell system consisting of a platinum plate, graphene deposited electrode, and Ag/AgCl (saturated with KCl) electrodes as the counter, working, and reference electrodes, respectively. The vertically aligned graphene was rinsed with ethanol and dried at room temperature for 1 h.

Characterization. Morphologies of all samples were observed by field effect scanning electron microscopy (FE-SEM, JEOL). Electrochemical properties for all vertical and stacked graphene samples on PSS were evaluated using a three-electrode cell system with a potentiostat (VSP, Princeton Applied Research, USA). A platinum plate (size: 1 cm^2) was used as a counter electrode, a Ag/AgCl (saturated with KCl) electrode was the reference, and all graphene/PSS samples used as working electrodes were immersed in PC electrolyte (Aldrich Inc.) containing 1 M $LiClO_4$. For measurement of the graphene layer, a quartz microbalance (QCM) (QCM922, Seiko Japan) and micro-Raman spectrometry were used to measure the weight of the graphene layer and the formation of graphene, respectively. The mass of the deposited material can be calculated from the following equation:[23]

$$\text{weight (g)} = \Delta\text{frequency}\cdot(-1.3)\ \text{ng/Hz} \quad (1)$$

A micro-Raman spectrometer with a 633 nm laser source (Renishaw, Germany) was used.

RESULTS AND DISCUSSION

Figure 1 shows schematic illustrations and scanning electron microscopy (SEM) images corresponding to the steps for vertical transformation of the graphene layers. Polystyrene sulfonate sodium salt (PSS-Na, Mw = 70 000, Aldrich) is first coated onto either a gold coated silicon wafer (200 nm thick, DC sputter; Q300T; Quorum Technologies Ltd.) or a gold plate (100 μm thick) using solution casting (Figure 1A-1). A top view SEM image of the PSS coated sample is shown in Figure 1A-2. To obtain high quality graphenes, expanded graphite (e-graphite; 200−300 μm flake size, ash content < 0.05 mass %, Zaval'evsk coal field, Ukraine) prepared by rapid thermal exfoliation was used. Graphene flakes doped with nitric acid (HNO_3, 63%, Daejung) treatment to introduce positive charges on their surfaces were dispersed in ethanol. They were spontaneously deposited on the PSS-Na layer due to the electrostatic interaction between positive charges on the graphene and negative charges on the PSS molecules, SO_3^- (Figure 1B-1). Planar graphene flakes of a few micrometers were uniformly coated on the PSS surface, as shown in Figure 1B-2. Using an electrochemical three-cell system with a platinum counter electrode, a Ag/AgCl reference electrode, and a gold coated silicon wafer as a working electrode, stacked graphenes on PSS were transformed into a vertical 3D shape. To transform the graphene geometry, an electric charge with constant potential (−2 V) and various currents (1−3 μAh/cm^2) were applied to the graphene layer. (Figure 1C) After the electric charge was applied, the graphene layer was rinsed with ethanol and dried at room temperature for 1 h. The notable finding from this study is that the geometries of the vertically

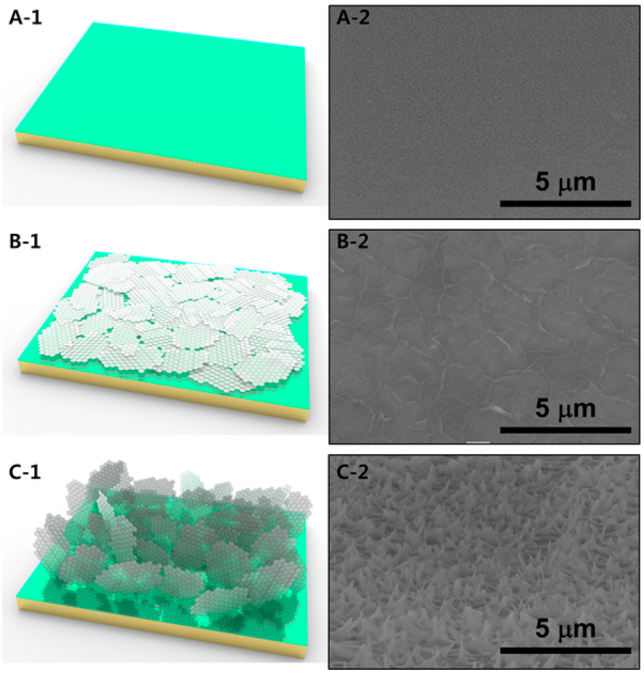

Figure 1. Schematic illustrations and SEM images corresponding to the steps for forming transformative vertical graphenes on PSS-Na coated Au thin films. (A) Spin-coated PSS-Na (Mw = 70 000) on Au coated wafer or Au foil. (B) Dip-coating graphene on PSS by electrostatic forces. (C) Vertical transformation of graphene by applying electric charge (−2 V with 3 μAh/cm^2) using a three-cell system.

transformed graphene layer are controlled by applied charges (Figure 2). For example, with a lower electrical charge (1 μAh/cm^2 at −2 V), as shown in Figure 2A, a few protruding graphenes (about 51% of the relative density; ratio of number of transformed graphenes to a maximum number of one) with relatively low standing angle can be found. When the electric charge is increased to 2 μAh/cm^2 at −2 V (Figure 2B), more graphenes (about 71% relative density) are gently transformed to a higher standing angle. With an electric charge of 3 μAh/cm^2 at −2 V, the SEM image in Figures 1C-2 and 2C clearly reveal most of the graphenes transformed vertically with much higher standing angles. The heights of the vertical graphene observed in SEM images are about 0.6−0.8 μm. As shown in Figure 2A,B,C, the densities of vertically standing graphenes are increased by increasing the applied electric charges and potentials in three cell systems (Figure 2D).

It is obvious that applied electric fields play a crucial role in the 3D transformation process of graphenes. We postulate that molecular transition of PSS induced by the applied potential is the major cause of the transformation.[24] It should be noted that PSS molecules can be extended by negative potentials and shrunk by positive potentials. Owing to underlying conductivity changes induced by extended or shrunk PSS chain conformations and the resulting accumulation of absorbed ion pairs on each graphene edge, graphenes have asymmetrical charges and eventually undergo shape transformation, as presented earlier with carbon nanotubes.[25−27] This phenomenon explains how applied potentials can modulate PSS chain shape and eventually result in asymmetrical charge accumulation as well as shape control of vertically aligned graphenes due to polarization of the graphene-edge along the direction of the electric field.

DOI: 10.1021/acsami.5b00630
ACS Appl. Mater. Interfaces 2015, 7, 8070−8075

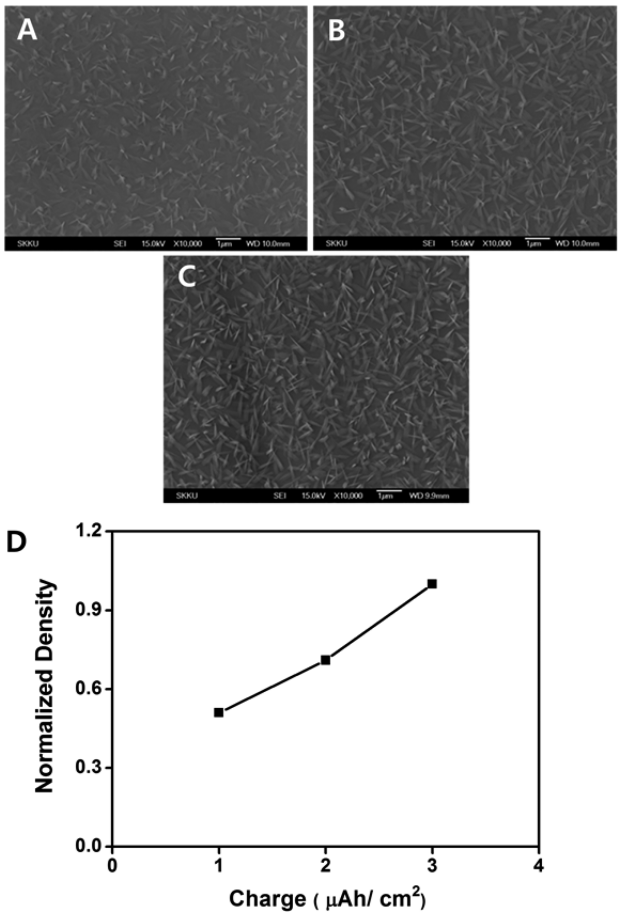

Figure 2. (A–C) SEM images of transformed graphenes by various applied charges, (A) 1, (B) 2, and (C) 3 μAh/cm^2 with −2 V potential, respectively. (D) Relative density of transformative graphenes by applied charges. All density values are normalized by dividing by the density of 3 μAh/cm^2 charge applied to the graphenes (as shown in Figure 1C).

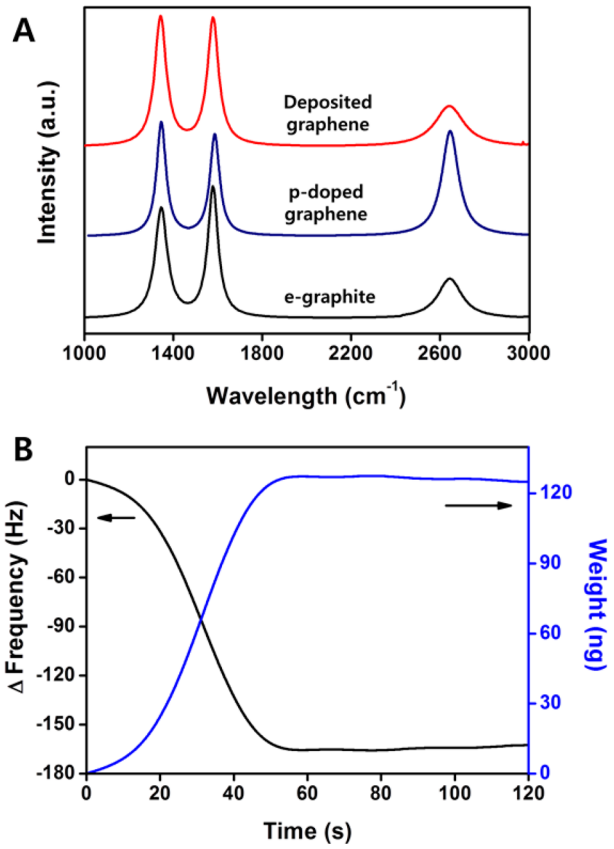

Figure 3. (A) Raman spectra of e-graphite, p-doped graphene, and deposited graphene with 633 nm laser source; (B) δ frequency change measured by quartz crystal microbalance (QCM) and weight changes of deposited graphenes by deposition time.

The deposited graphenes were confirmed by Raman spectroscopy. Figure 3A shows Raman peak comparisons between the Raman spectra of e-graphite, p-doped graphene, and deposited graphene on PSS-Na film. The D, G, and 2D peaks of e-graphite can be observed at 1344, 1577, and 2641 cm^{-1}, respectively. The spectra correspond well with those reported for e-graphite prepared by a thermal expansion method.[28] Generally, the 2D peak in graphite consists of two components, $2D_1$ and $2D_2$. In this case, the graphite was significantly expanded by thermal shock, therefore the 2D peak of e-graphite behaves like multilayer graphene. For doped graphene, the D, G, and 2D peaks are shifted toward higher wavenumbers: 1345, 1585, and 2642 cm^{-1}, respectively. This result is similar to those obtained by others.[29] The 2D/G ratio of intensity, I (2D/G), is related to the number of graphene layers, with a graphene monolayer having the maximum value. The I (2D/G) of p-doped graphene was enhanced from 0.37 to 0.98, an indication that the doped graphite was exfoliated by sonication and existed as a bilayer in the electrolyte.[30] After deposition, the D, G, and 2D peaks were observed at 1344, 1577, and 2641 cm^{-1} respectively. The p-doped graphene was reduced by negative charges on the surface of the PSS film and the peaks shifted to the left side. From the well-defined single 2D peak and 0.30 ratio of the I (2D/G) peaks, the deposited graphenes existed as multilayer on PSS film.

The deposition of p-doped graphene on PSS-Na film was monitored by quartz crystal microbalance (QCM). Figure 3B shows the deposited graphene mass change on PSS film as a function of deposition time. The graph shows a linear time-dependent deposition rate (~2 ng/s) in the first 60 s and a constant rate after that. It indicates that electrostatic interaction between PSS and graphene is dominant at only a certain thickness of the deposited graphene layer due to limited interaction length. As a result, we were able to estimate the

Table 1. Results for Graphene Deposition and Transformation on Various Polymers

bottom layer	polarity of functional group	electrostatic deposition	electrophoresis deposition	3D transformation
polyvinylidene fluoride (PVDF)		X	X	X
polystyrene (PS)		X	X	X
polyacrylic acid (PAA)	COO^-	O	X	X
Nafion	SO_3^-	O	X	X
PSS-Na	SO_3^-	O	X	O

DOI: 10.1021/acsami.5b00630
ACS Appl. Mater. Interfaces 2015, 7, 8070–8075

overall weight of deposited graphene as approximately 0.78 μg/cm^2 in a 0.28 cm^2 lateral dimension of gold coated substrate. As shown in Figure S1 in the Supporting Information, the δ frequency and mass of 2D stacked graphenes and vertically transformed graphenes measured by QCM did not change even while electrical charge was applied.

We found that deposition of graphene is strongly dependent on the chemical polarity of underlying materials. Table 1 shows various types of underlying polymers and their functional groups. Polyvinylidene fluoride (PVDF, Mw = 534 000, Aldrich), polystyrene (PS, Mw = 3000, Aldrich), Nafion (Dupont Inc.), and Polyacrylic acid (PAA, Mw = 100 000, Aldrich) were tested with electrophoresis or electrostatic deposition methods. Notably, graphenes can be deposited on ion-conductive polymers with a negative polarity functional group such as PSS and Nafion with SO_3^- and PAA. From our experimental results, however, Nafion and PAA have weak or no chain deformations and shape deformations of graphene on such polymers are undetectable.

As shown in Figure 4A, cyclic voltammograms of vertical graphene had larger areas and higher current densities, which explain the higher capacitance and smaller internal resistance generated by vertical graphene. Specific capacitance of the 3D vertically aligned graphenes transformed by 3 μAh/cm^2 with −2 V was 410 F g^{-1}, over 4 times higher than that of planar graphene. These exceed the best values of up to 250 F g^{-1} obtained for graphene based supercapacitors in aqueous systems. Also, we were able to get areal capacitance, 319.8 μF/cm^2 that is much higher value compared to the areal capacitance of the thin graphene film reported recently (80 μF/cm^2).[31] However, loss of charge propagation was observed from the nonrectangular shape of cyclic voltammograms as a result of the poor conductivity of PSS-Na and the experiments were performed in an organic system.

A comparison of capacitive performance between planar and vertical graphene was further performed using cyclic voltammetry in the range from −1 to 0 V as a function of scan rate (in Figure 4B). The scanning range from −1 to 0 V is lower than −2 V, the threshold voltage for graphene transformation; it is useful to measure specific capacitance property without change of graphene morphology. The specific capacitance property was calculated by integrating the area under the cyclic voltammograms and normalized by the measured weight. The capacitances of both graphene slightly decreased when the scan rate was increased to as high as 1000 mV s^{-1}. At a high scan rate, capacitance is generally limited by charge propagation.[32] The vertical graphene maintained its 87.48% capacitance (358.69 F g^{-1}) as the scan rate was increased from 100 to 1000 mV s^{-1}, whereas the flat graphene retained only 61.7% of its capacity in the same scan rate range.

Edge site performance of graphene has been studied for use with supercapacitors because the edge site has better electrochemical properties than the basal plane.[33] Generally, charge storage occurs on the edge planes of graphene that are exposed and directly accessible. Edge sites in graphene accelerate the movement of the charge generated at the interface between the electrolyte and electrode and store more charge through additional surface redox reactions similar to a pseudocapacitor.[34] Ambrosi et al. reported on the electrochemical properties of the edge of graphene, stating that edge sites of graphene provide not only much higher capacitance but also 35 times faster electron transfer rate than the basal plane of graphene.[33] Furthermore, vertically aligned graphene allows for minimized

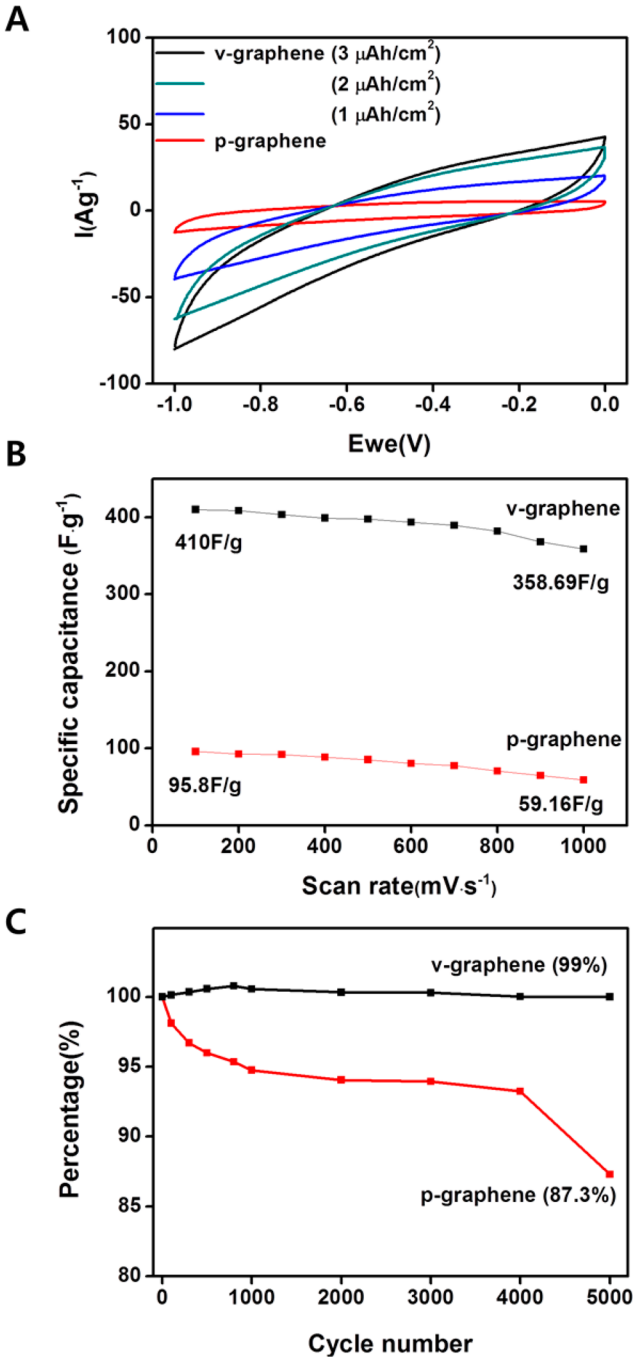

Figure 4. (A) Cyclic voltammograms plot for the specific capacitance variations of 2D stacked (planar) graphene (p-graphene) (red), transformed graphenes with applying potentials at −2 V with 1 (blue), 2 (green), and 3 (v-graphene; black) μAh/cm^2 in HNO_3/ethanol (pH 4.0) electrolyte. (B) Specific capacitances of 2D stacked graphene and 3D transformed graphene as a function of scan rate. (C) Specific capacitances of 2D stacked graphene and 3D transformed graphene as a function of cycle-number (characterized at scan rate of 300 mV s^{-1}).

porosity effects because of its open structure, reducing ionic resistance.[33] It is obvious that vertically aligned graphene provide a pathway to store more charge and facilitate high rate performance by increasing the number of edge sites exposed to electrolytes. Cyclic stability test was also conducted at a scan rate of 100 mV s^{-1}, and vertical graphene showed no degradation in performance after 5000 cycles (for 27.7 h) whereas planar graphene showed a decrease in capacitance to

DOI: 10.1021/acsami.5b00630
ACS Appl. Mater. Interfaces 2015, 7, 8070−8075

87.3%. (Figure 4C) We postulate the vertically aligned graphene electrodes allow open structures and enhanced area of graphene edges to have high stability against volume expansion induced by repeated cyclic tests.

CONCLUSION

In summary, we have presented a facile fabrication method to achieve 3D transformative graphenes in a geometry controllable manner by applying low potential and have also presented its electrochemical characterizations as a supercapacitor. The angle and density of vertical transformed graphenes can be minutely controlled. Electrochemical analysis with current−time and cyclic voltammograms show that 3D transformed graphenes offer improved results over 2D stacked graphenes. The capacitance of the 3D graphene was 403 F g^{-1} after 5000 cycles with a scan rate of 300 mV s^{-1}, which is significantly improved compared to 80.2 F g^{-1} of 2D stacked graphene under the same conditions. We believe that this work provides a remarkable pathway to achieving hierarchical, vertical structures using 2D materials. It would be reasonable to expect that this method can be used as a powerful electrochemical technique to manipulate the structure of graphene for supercapacitors or other relevant electronic devices.

ASSOCIATED CONTENT

Supporting Information

QCM results of deposited graphene and cyclic voltammetry characteristics of planar and vertical graphenes. This material is available free of charge via the Internet at http://pubs.acs.org.

AUTHOR INFORMATION

Corresponding Authors

*Prof. T.-i. Kim. Email: taeilkim@skku.edu. Tel.: +82 31 290 7312.

*Prof. Y. Lee. Email: yklee@skku.edu. Tel.: +82 31 290 7326.

Author Contributions

⊥These authors contributed equally.

Notes

The authors declare no competing financial interest.

ACKNOWLEDGMENTS

This research was done in KANEKA/SKKU Incubation Center and financially supported by Kaneka Corp. in Japan, and was supported by Energy Efficiency & Resources of the Korea Institute of Energy Technology Evaluation and Planning (KETEP) grant funded by the Korea government Ministry of Knowledge Economy (No. 20142010102690). The work also supported by Basic Science Research Program through the National Research Foundation of Korea (NRF) funded by the Ministry of Education, Science and Technology (2009-0083540), NRF-2013-R1A1A1061403, and the Pioneer Research Center Program (NRF-2014M3C1A3001208) and by IBS-R015-D1.

REFERENCES

(1) Hou, Z.-L.; Song, W.-L.; Wang, P.; Meziani, M. J.; Kong, C. Y.; Anderson, A.; Maimaiti, H.; LeCroy, G. E.; Qian, H.; Sun, Y.-P. Flexible Graphene−Graphene Composites of Superior Thermal and Electrical Transport Properties. *ACS Appl. Mater. Interfaces* **2014**, *6*, 15026−15032.

(2) Lee, W. J.; Maiti, U. N.; Lee, J. M.; Lim, J.; Han, T. H.; Kim, S. O. Nitrogen-Doped Carbon Nanotubes and Graphene Composite Structures for Energy and Catalytic Applications. *Chem. Commun.* **2014**, *50*, 6818−6830.

(3) Lee, S. H.; Lee, D. H.; Lee, W. J.; Kim, S. O. Tailored Assembly of Carbon Nanotubes and Graphene. *Adv. Funct. Mater.* **2011**, *21*, 1338−1354.

(4) Novoselov, K. S.; Jiang, D.; Schedin, F.; Booth, T. J.; Khotkevich, V. V.; Morozov, S. V.; Geim, A. K. Two-Dimensional Atomic Crystals. *Proc. Natl. Acad. Sci. U. S. A.* **2005**, *102*, 10451−10453.

(5) Sun, P.; Zhu, M.; Wang, K.; Zhong, M.; Wei, J.; Wu, D.; Zhu, H. Small Temperature Coefficient of Resistivity of Graphene/Graphene Oxide Hybrid Membranes. *ACS Appl. Mater. Interfaces* **2013**, *5*, 9563−9571.

(6) Eda, G.; Fanchini, G.; Chhowalla, M. Large-Area Ultrathin Films of Reduced Graphene Oxide as a Transparent and Flexible Electronic Material. *Nat. Nanotechol.* **2008**, *3*, 270−274.

(7) Moon, I. K.; Lee, J.; Ruoff, R. S.; Lee, H. Reduced Graphene Oxide by Chemical Graphitization. *Nat. Commun.* **2010**, *1*, 73.

(8) Hao, Y.; Bharathi, M. S.; Wang, L.; Liu, Y.; Chen, H.; Nie, S.; Wang, X.; Chou, H.; Tan, C.; Fallahazad, B.; Ramanarayan, H.; Magnuson, C. W.; Tutuc, E.; Yakobson, B. I.; McCarty, K. F.; Zhang, Y.-W.; Kim, P.; Hone, J.; Colombo, L.; Ruoff, R. S. The Role of Surface Oxygen in the Growth of Large Single-Crystal Graphene on Copper. *Science* **2013**, *342*, 720−723.

(9) Bae, S.; Kim, H.; Lee, Y.; Xu, X.; Park, J.-S.; Zheng, Y.; Balakrishnan, J.; Lei, T.; Kim, H. R.; Song, Y. I.; Kim, Y.-J.; Kim, K. S.; Ozyimaz, B.; Ahn, J.-H.; Hong, B. H.; Iijima, S. Roll-to-Roll Production of 30-Inch Graphene Films for Transparent Electrodes. *Nat. Nanotechnol.* **2010**, *5*, 574−578.

(10) Lee, S.-K.; Kim, B. J.; Jang, H.; Yoon, S. C.; Lee, C.; Hong, B. H.; Rogers, J. A.; Cho, J. H.; Ahn, J. H. Stretchable Graphene Transistors with Printed Dielectrics and Gate Electrodes. *Nano Lett.* **2011**, *11*, 4642−4646.

(11) Wang, H.; Yang, Y.; Liang, Y.; Robinson, J. T.; Li, Y.; Jackson, A.; Cui, Y.; Dai, H. Graphene-Wrapped Sulfur Particles as a Rechargeable Lithium−Sulfur Battery Cathode Material with High Capacity and Cycling Stability. *Nano Lett.* **2011**, *11*, 2644−2647.

(12) Gong, Y.; Yan, S.; Zhan, L.; Ma, L.; Vajtai, R.; Ajayan, P. M. A Bottom-up Approach to Build 3D Architectures from Nanosheets for Superior Lithium Storage. *Adv. Funct. Mater.* **2014**, *24*, 125−130.

(13) Maiti, U. N.; Lee, W. J.; Lee, J. M.; Oh, Y.; Kim, J. Y.; Kim, J. E.; Shim, J.; Han, T. H.; Kim, S. O. 25th Anniversary Article: Chemically Modified/Doped Carbon Nanotubes & Graphene for Optimized Nanostructures & Nanodevices. *Adv. Mater.* **2014**, *26*, 40−67.

(14) Lee, S. H.; Kim, H. W.; Hwang, J. O.; Lee, W. J.; Kwon, J.; Bielawski, C. W.; Ruoff, R. S.; Kim, S. O. Three-Dimensional Self-Assembly of Graphene Oxide Platelets into Mechanically Flexible Macroporous Carbon Films. *Angew. Chem., Int. Ed.* **2010**, *49*, 10084−10088.

(15) Wang, H.; Sun, K.; Tao, F.; Stacchiola, D. J.; Hu, Y. H. 3D Honeycomb-like Structured Graphene and Its High Efficiency as a Counter-Electrode Catalyst for Dye-Sensitized Solar Cells. *Angew. Chem., Int. Ed.* **2013**, *52*, 9210−9214.

(16) Yavari, F.; Chen, Z.; Thomas, A. V.; Ren, W.; Cheng, H.-W.; Koratkar, N. High Sensitivity Gas Detection Using a Macroscopic Three-Dimensional Graphene Foam Network. *Sci. Rep.* **2011**, *1*, No. 166, DOI: 10.1038/srep00166.

(17) Dong, L.; Chen, Z.; Yang, D.; Lu, H. Hierarchically Structured Graphene-based Supercapacitor Electrodes. *RSC Adv.* **2013**, *3*, 21183−21191.

(18) Yu, D.; Goh, K.; Wang, H. W.; Wei, L.; Jiang, W.; Zhang, Q.; Dai, L.; Chen, Y. Scalable Synthesis of Hierarchically Structured Carbon Nanotube−Graphene Fibres for Capacitive Energy Storage. *Nat. Nanotechnol.* **2014**, *9*, 555−562.

(19) Yoon, Y.; Lee, K.; Kwon, S.; Seo, S.; Yoo, H.; Kim, S.; Shin, Y.; Park, Y.; Kim, D.; Choi, J.-Y.; Lee, H. Vertical Alignments of Graphene Sheets Spatially and Densely Piled for Fast Ion Diffusion in Compact Supercapacitors. *ACS Nano* **2014**, *8*, 4580−4590.

(20) Xu, P.; Kang, J.; Choi, J.-B.; Surh, J.; Yu, J.; Li, F.; Byun, J.-H.; Kim, B.-S.; Chou, T.-W. Laminated Ultrathin Chemical Vapor

DOI: 10.1021/acsami.5b00630
ACS Appl. Mater. Interfaces 2015, 7, 8070−8075

Deposition Graphene Films based Stretchable and Transparent High-Rate Supercapacitor. *ACS Nano* **2014**, *8*, 9437−9445.
(21) Maiti, U. N.; Lim, J.; Lee, K. E.; Lee, W. J.; Kim, S. O. Three-Dimensional Shape Engineered, Interfacial Gelation of Reduced Graphene Oxide for High Rate, Large Capacity Supercapacitors. *Adv. Mater.* **2014**, *26*, 615−619.
(22) Lee, J. H.; Shin, D. W.; Makotchenko, V. G.; Nazarov, A. S.; Fedorov, V. E.; Kim, Y. H.; Choi, J.-Y.; Kim, J. M.; Yoo, J.-B. One-Step Exfoliation Synthesis of Easily Soluble Graphite and Transparent Conducting Graphene Sheets. *Adv. Mater.* **2009**, *21*, 4383−4387.
(23) Lee, S.; Cho, M. S.; Lee, H.; Nam, J.-D.; Lee, Y. A Facile Synthetic Route for Well Defined Multilayer Films of Graphene and PEDOT via an Electrochemical Method. *J. Mater. Chem.* **2012**, *22*, 1899.
(24) Kawaguchi, M.; Hayashi, K.; Takahashi, A. Effect of Applied Potential on the Ellipsometric Thickness of Sodium Poly-(styrenesulfonates) Adsorbed on a Platinum Surface. *Macromolecules* **1988**, *21*, 1016−1020.
(25) Chan, R. H. M.; Fung, C. K. H.; Li, W. J. Rapid Assembly of Carbon Nanotubes for Nanosensing by Dielectrophoretic Force. *Nanotechnology* **2004**, *15*, No. S672.
(26) Nagahara, L. A.; Amlani, I.; Lewenstein, J.; Tsui, R. K. Directed Placement of Suspended Carbon Nanotubes for Nanometer-Scale Assembly. *Appl. Phys. Lett.* **2002**, *80*, 3826.
(27) Krupke, R.; Hennrich, F.; Löhneysen, H. V.; Kappes, M. M. Separation of Metallic from Semiconducting Single-Walled Carbon Nanotubes. *Science* **2003**, *301*, 344−347.
(28) Ferrari, A. C.; Meyer, J. C.; Scardaci, V.; Casiraghi, C.; Lazzeri, M.; Mauri, F.; Piscanec, S.; Jiang, D.; Novoselov, K. S.; Roth, S.; Geim, A. K. Raman Spectrum of Graphene and Graphene Layers. *Phys. Rev. Lett.* **2006**, *97*, 187401.
(29) Kudin, K. N.; Ozbas, B.; Schniepp, H. C.; Prud'homme, R. K.; Aksay, I. A.; Car, R. Raman Spectra of Graphite Oxide and Functionalized Graphene Sheets. *Nano Lett.* **2008**, *8*, 36−41.
(30) Jung, N.; Kim, N.; Jockusch, S.; Turro, N. J.; Kim, P.; Brus, L. Charge Transfer Chemical Doping of Few Layer Graphenes: Charge Distribution and Band Gap Formation. *Nano Lett.* **2009**, *9*, 4133−4137.
(31) Yoo, J. J.; Balakrishnan, K.; Huang, J.; Meunier, V.; Sumpter, B. G.; Srivastava, A.; Conway, M.; Reddy, A. L. M.; Yu, J.; Vajtai, R.; Ajayan, P. M. Ultrathin Planar Graphene Supercapacitors. *Nano Lett.* **2011**, *11*, 1423−1427.
(32) Kötz, R.; Carlenb, M. Principles and Applications of Electrochemical Capacitors. *Electrochim. Acta* **2000**, *45*, 2483−2498.
(33) Miller, J. R.; Outlaw, R. A.; Holloway, B. C. Graphene Double-Layer Capacitor with ac Line-Filtering Performance. *Science* **2010**, *329*, 1637−1639.
(34) Qu, D. Studies of the Activated Carbons Used in Double-Layer Supercapacitors. *J. Power Sources* **2002**, *109*, 403−411.

DOI: 10.1021/acsami.5b00630
ACS Appl. Mater. Interfaces 2015, 7, 8070−8075